

# Lattice Dynamics of Boron Phosphide

H. W. Leite Alves

*Departamento de Ciências Naturais - FUNREI, Fundação de Ensino Superior de São João del Rei  
Praça D. Helvécio, 74, 36300-000, São João del Rei, MG, Brasil*

and

K. Kunc

*Laboratoire de Physique des Solides, associé au CNRS  
Université P. et M. Curie 4, pl. Jussieu, Tour 13  
75252 Paris-Cedes 05, France*

Received July 12, 1993

Using the density-functional theory, norm-conserving pseudopotentials and plane-wave expansions, we have calculated ab initio the equation of state and the principal phonon modes in Boron Phosphide, including their pressure dependence and the amplitude of the eigendisplacements. A good agreement with the experiment is obtained, whenever a comparison is possible: in fact, most of the results are predictions. A 10-parameter Valence Overlap Shell Model is then constructed from the available experimental data, which are completed by the data obtained in the first-principle calculations: frozen phonon frequencies and eigenvectors. The previous speculations about the anomalous behavior of the effective charges are discussed in the context of the present results.

## I. Introduction

Actually, there has been considerable interest in the developing optoelectronic and microelectronic devices which work under hard conditions such as high temperatures or aggressive environment. One of the promising materials for this purpose is Boron Phosphide since these conditions were satisfied by its physical properties, such as hardness, high melting point and resistance to corrosion<sup>[1,2]</sup>. Unfortunately, the amount of theoretical knowledge on this substance is limited to a handful of works<sup>[3-6]</sup> and, particularly, the data on phonon spectra and vibrational properties are rather scarce<sup>[7,8]</sup>.

Under normal conditions, the BP appears in zinc-blende structure and shows an indirect  $\Gamma - X$  gap of 2.4 eV. The calculations in Ref. 3 and Ref. 6 revealed that the calculated charge distribution differs from the usual III-V picture characterized by a large accumulation of the electronic charge around the anion, in BP the strongly attractive B potential causes a nearly symmetrical distribution of the valence charge

between the cation and the anion, reminiscent of homopolar bonding; the small heteropolarity is thus consequence of the strong electronegativity of the B atoms. This could explain its hardness. It was also noticed<sup>[4]</sup> that at high pressures this homopolarity is enhanced. According to the experiment<sup>[8]</sup>, the transverse effective charges ( $e_T^*$ ) associated with the atoms decrease with increasing pressure. Despite the experiment is not capable to precise the sign of  $e_T^*$ , Sanjurjo et al<sup>[8]</sup> deduced, from BP pseudopotential form factors evaluation, that this sign is negative since the BP polarity is close to zero.

As the electronic and structural properties of BP were already addressed<sup>[3-6]</sup> within the Density Functional Theory<sup>[9]</sup> in the Local Density Approximation(LDA), we have applied the same approach to calculate the total energy in order to supply the missing experimental information on the vibrational properties of BP in the zinc-blende modification. Norm-conserving pseudopotentials<sup>[10]</sup> are used, together with plane-wave expansions, and the Ceperley-

Alder exchange-correlation<sup>[11]</sup> is adopted. Following the procedures summarized e.g. in Ref. 12 we start by checking the lattice parameter  $a_0$ , bulk modulus  $B_0$  and its pressure derivative  $B'_0$  as well as the electronic charge distribution  $n(\mathbf{r})$  in Section II, and calculate the frequencies and eigenvectors of selected phonons in Section III. A construction of a simple mechanical model (Valence Overlap Shell Model (VOSM))<sup>[13]</sup> is then attempted in Section IV, which accounts, in terms of 10 parameters, for all the calculated frequencies and eigenvectors, as well as for all the available experimental data (such as the elastic constants, and the  $TO(\Gamma)$  and  $LO(\Gamma)$  frequencies). The question of the sign of the effective charges of  $\text{In}$  and  $\text{P}$  is raised and briefly discussed in Section V. The main results are summarized in Section VI.

## II. Equilibrium properties

Our first step consists in verifying that our calculational procedure correctly describes the undistorted structure in static equilibrium. We have evaluated the total energy for various values of the lattice constant, at different plane-wave energy cut-offs and numbers of k-points sampled in the irreducible Brillouin zone. Our results were described in Ref. 6 and is summarised in Table 1, for cut-off energies varying from  $E_{pw} = 12$  Ry to 27 Ry.

The results obtained for the lattice constant ( $a_0 = 4.52\text{\AA}$ ), Bulk Modulus ( $B_0 = 1.67$  Mbar) and its pressure derivative ( $B'_0 = 3.3$ ) are in good agreement with the available experimental results<sup>[14,15]</sup> (0.5% to 3.5% of error), as well as with the previous calculations<sup>[3]</sup> in which  $a_0 = 4.56\text{\AA}$  and  $B_0 = 1.65$  Mbar was obtained. We also verified that our calculated LDA-band structure agrees with that found in Ref. 3: our calculated full valence bandwidth of 15.7 eV and direct gap of 3.34 eV, compare well with 15.3 eV and 3.3 eV of Ref. 3. We also obtained an indirect gap of 1.01 eV at

Table 1: Convergence of the calculated static properties of zinc-blende BP with energy cut-offs of the plane-wave expansion and with the number of k-points in the Brillouin zone sampling.

$E_{pw}$ (Ry)	$n^{\ominus}$ k-points	$a_0$ ( $\text{\AA}$ )	$B_0$ (Mbar)	$B'_0$
12	2	4.860	0.33	6.11
15	2	4.574	1.80	3.11
18	2	4.549	1.71	3.17
21	2	4.530	1.82	2.74
24	2	4.522	1.65	<b>3.33</b>
27	2	4.514	1.72	3.14
12	10	4.652	1.61	2.94
15	10	4.574	1.82	3.12
18	10	4.543	1.68	3.29
21	10	4.526	1.70	3.22
24	10	4.517	1.67	3.28
experiment:		4.538	1.73	Ref.14
			2.67	Ref.15

$\Delta_{\min} = 2\pi/a_0 (0,0,0.84)$  which is close to 1.2 eV, found in the previous calculations<sup>[3]</sup>.

The real-space distribution of the electronic charge density  $n(\mathbf{r})$  shown in Fig. 1 agrees with the previous calculations<sup>[3]</sup> as well: it is immediately apparent from the contour plot that the valence charge distribution in BP differs considerably from that of typical 111-V semiconductors<sup>[16]</sup>, viz. by showing a significant bond charge between the atoms, which suggests the idea of rather a covalent than ionic bonding.

## III. Frozen phonons

The phonon frequencies and the respective eigenvectors of the vibrations at the high symmetry points in the Brillouin zone were calculated by the well known "frozen phonon" method<sup>[12]</sup>: the frequency of the phonon is obtained from the difference of the total energies between the undisplaced structure and the structure with atoms displaced in the particular phonon mode. In this way, we evaluated the eigenfrequencies and eigenvectors of the  $TO(\Gamma)$ ,  $LO(X)$ ,  $LA(X)$ ,  $TO(X)$ ,  $TA(X)$ ,  $LO(L)$  and  $LA(L)$  phonons. For most of the

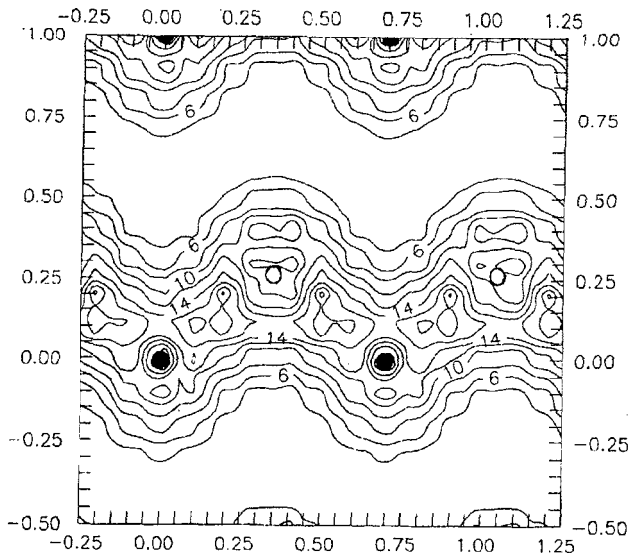


Figure 1: Pseudo-charge density for zinc-blende BP in static equilibrium calculated in the (1 1 0) plane. The unit of length is the lattice constant  $a$  and the contour interval is 2 electrons/cell. The full circles are the B atoms while the open ones are the P atoms.

zone-boundary phonons one also has to determine the actual displacement patterns - the procedure was described further in<sup>[12,17,20]</sup>; the results are summarized in Table 2.

The ab initio calculations have much to offer in this area since very little experimental work exists for this material. The only data which can be compared with our calculations are the phonon frequency  $\nu$  and the Grüneisen parameter  $\gamma$  for the TO mode at  $\Gamma$  obtained by Raman measurements<sup>[7]</sup> which are, respectively, 23.95 THz and 1.3, and with which our calculated values, 24.25 THz and 1.14, agree to within +4% and -12%.

For the longitudinal phonons, the displacement patterns consist in oscillations of either the B or P sublattices alone<sup>[17]</sup>. The difference between the masses of B and P is so large that even without the energy calculations we can identify the LO mode with the displacements of the B sublattice (the lighter atoms) and the LA mode with the P atoms oscillations. These displacement patterns were, indeed, confirmed by our calculations in the same way as they were verified earlier

Table 2: Summary of the most important phonon frequencies with their respective Grüneisen parameters  $\gamma$  calculated ab initio. The results given here were obtained with the cut-off energy of 21 Ry in the plane-wave expansions.

Phonon mode	$\nu$ (THz)	$\gamma$	$n^{\circ}$ k-points
TO( $\Gamma$ )	24.25	1.14	5
LO(X)	24.00	0.90	3
LA(X)	13.81	0.94	3
TO(X)	21.04	1.54	4
TA(X)	9.20	-0.27	4
LO(L)	22.91	1.03	12
LA(L)	15.18	1.00	12
exp.: TO( $\Gamma$ )	23.95	1.30	Ref.8

in GaP<sup>[18]</sup>.

For the transverse phonons at X and for the phonon modes at L we know that we can treat these modes as coupled oscillations of displacement patterns  $S_1$  and  $S_2$  which correspond to the respective phonon modes in the diamond structure. We proceed, then, as in the previous works<sup>[19,20]</sup>, and evaluate the right linear combination of these displacement patterns by diagonalizing the  $2 \times 2$  matrices of the coupling coefficients. The convergence of the calculated frequencies of the zone-boundary phonons (LO(X), LA(X), TO(X), TA(X), LO(L) and LA(L)) with the plane-wave energy cut-off is described in Ref. 6, but their frequencies and Grüneisen parameters are summarized here in Table 2.

There are no experimental data for these modes in BP and our calculations present an attempt to supply the missing information. We observe that, as in other III-V compounds, the TA(X) is a soft mode and its frequency decreases with increasing pressure: the Grüneisen parameter  $\gamma$  has a negative value.

When the problem of coupled oscillations ( $S_1, S_2$ ) is solved<sup>[18,19]</sup>, the resulting linear combination of the displacement patterns provides us with information about the eigenvectors of each vibrational mode. For eigenvectors of the LO(L) and LA(L) phonon modes, the calculated atomic displacement  $|u_1/u_2|$  ratios (1 refers

to B and 2 to P) approach the values which mean, practically,  $\infty$  and 0 - although no symmetry argument requires one sublattice to vibrate and the other to be at rest. We note that similar result was obtained in SiC<sup>[20]</sup> as well, and is, probably, due to the large difference in the masses of the two atoms. All calculated values of the eigenvectors are given in the last column of the Table 4.

#### IV. Shell model

The most widely used among the different mechanical models of interatomic interaction in semiconductor compounds has been the well known shell model of Dick and Overhauser<sup>[21]</sup> and Cochran<sup>[22]</sup>. In this model, the ions are assumed to be polarizable and mechanically deformable and the atomic vibrations are described as motion of a system of *cores* and massless, charged *shells*, bound to the respective *cores* by harmonic springs; the *cores* are connected with each other, in the most general case, by tensor forces. The vibrations then cause polarization and deformation of the electrostatic charge distribution in a crystal, which is modelled as relative displacements of the *shells*.

The particular version of the shell model we use is known<sup>[13]</sup> as Valence Overlap Shell Model (VOSM): all the generalised forces are assumed to have the form of a "Valence Force Field". In this work, the 10 model parameters were fitted, by a non-linear least-squares method with constrained parameters and weighting, to all of the available information about phonon frequencies, elastic constants and eigenvectors at X and L. In other words, to the set of phonon frequencies evaluated by the frozen phonon method in the previous section, we are adding the experimental values of the TO( $\Gamma$ ) and LO( $\Gamma$ ) frequencies and of the elastic constants  $c_{11}$ ,  $c_{12}$  and  $c_{44}$ . In addition, we also have included in the minimized sum of squares the data on the eigendisplacements, i.e., the ratio of the amplitudes  $u_1/u_2$  for the

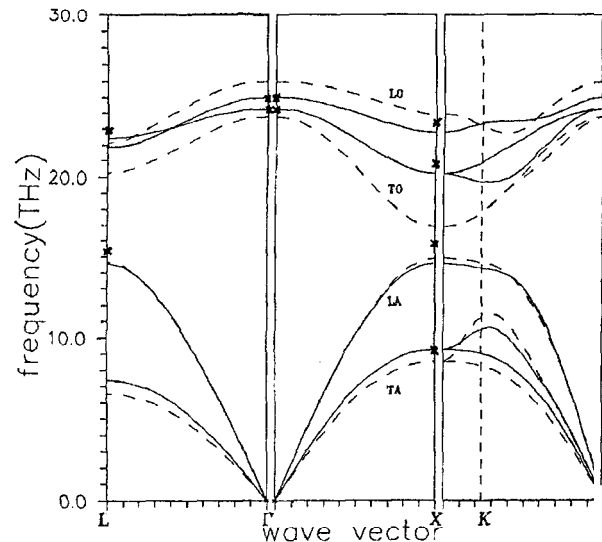


Figure 2: Phonon dispersion curves of zinc-blende BP calculated by VOSM: the dashed lines correspond to the initial guess and the solid lines were obtained from the final set of parameters (row (b) of Table 3). The asterisks are the experimental and the ab initio results.

transverse modes at X and the longitudinal modes at L, as well as the information on which sublattice moves in the longitudinal modes at X. The fitting process follows closely the procedure developed in<sup>[20]</sup> in which the same ideas were applied to SiC.

The details of this fitting procedure are described in Ref. 6. In Table 3 we summarize the model parameters obtained by the fitting procedure: the initial set of parameters (row (a)) and the final set (row (b)); the resulting frequencies and displacements are shown in Table 4 and in figure 2. The calculated phonon dispersion (fig. 2) shows the same general features as other III-V semiconductor compounds<sup>[23]</sup>.

In Table 4, the phonon frequencies and eigendisplacements at the high symmetry points calculated by VOSM, are compared with those obtained in the ab initio calculations, as well as with the experimental values, whenever available. The final results show, in general, a good agreement in frequencies (5% of deviation); as for the displacements, we note that, despite their inclusion in the fitting procedure, the eigenvectors of the TO(X) phonon and LO(L), LA(L) are only imperfectly reproduced. The calculated elastic con-

Table 3: Parameters of the VOSM for BP: (a) the initial guess obtained by mass approximation on the parameters of GaP (Ref. 12); (b) the final set of parameters. All parameters are in  $e^2/v_a$  units, with  $v_a = a_0^3/4$  and  $a_0 = 4.52\text{\AA}$ , except the charges  $Z_1$ ,  $Y_1$  and  $Y_2$  which are in atomic units.

	$\lambda$	$k_\theta$	$k'_\theta$	$k_{r\theta}$	$k'_{r\theta}$	$Z_1$	$Y_1$	$Y_2$	$K_1$	$K_2$
(a)	47.5	-1.15	-0.31	4.61	-7.06	2.00	6.03	-1.87	371.2	82.00
(b)	46.2	0.88	-2.07	4.95	-7.50	2.14	5.15	-2.97	296.9	80.81

Table 4: Phonon frequencies and eigendisplacements at high-symmetry points of the Brillouin zone calculated by the VOSM with the parameters listed in Table 3.

	(a)		(b)		LDF. cal		exp.[8]
	$\nu(\text{THz})$	$ u(B)/u(P) $	$\nu(\text{THz})$	$ u(B)/u(P) $	$\nu(\text{THz})$	$ u(B)/u(P) $	$\nu(\text{THz})$
LO( $\Gamma$ )	26.00	2.87	25.04	1.24			24.90
TO( $\Gamma$ )	23.76	2.87	24.28	1.24	24.25		23.95
LO(X)	23.94	$\infty$	22.83	$\infty$	24.00	$\infty$	
LA(X)	14.90	0	14.57	0	15.81	0	
TO(X)	16.40	0.92	20.27	1.09	21.04	3.59	
TA(X)	8.53	0.94	9.25	0.81	9.20	0.80	
LO(L)	22.12	109.88	21.81	11.01	22.91	94.51	
LA(L)	14.66	0.03	14.58	0.26	15.18	0.03	
TO(L)	20.27	0.85	22.46	2.58			
TA(L)	6.54	0.83	7.40	0.70			

stants ( $c_{11} = 31.33 \times 10^{11}$ ,  $c_{12} = 10.26 \times 10^{11}$  and  $c_{44} = 15.39 \times 10^{11}$  dyn/cm $^{-3}$ ) agree with the experimental ones<sup>[14]</sup> to within  $\approx 4\%$ .

## V. Effective charges

As we seen in the previous sections, the electronic charge distribution in BP differs from the usual III-V compounds because its density is nearly symmetrically distributed between the cation and the anion. In view of the strong electronegativity of the B atoms, speculations arise about the sign of the effective charges in BP, which are determined by Raman spectroscopy or infrared absorption, only in absolute value: it was suggested that, contrary to the usual "polarity", the effective charges of B might be negative and those of P positive.

We thus attempted to evaluate the effective charges *ab initio*, by proceeding exactly as in Ref. 12: we have used a tetragonal cell of BP which was six times the size of the primitive cell (volume:  $6a_0^3/4$ ), and accomplished 3 self-consistent calculations: one with all the atoms in

their equilibrium position and two with only one atomic plane (B or P) displaced by  $\vec{u} = 0.005a_0(1,0,0)$ . The screened Hartree potential was averaged in the planes perpendicular to the  $[1\ 0\ 0]$  direction, and from the slope of its variation with  $x$  we obtained the longitudinal effective charge  $e_L^*$ . On the other hand, from the Hellmann-Feynman forces acting on the atoms in the center of the supercell, we calculated the transverse effective charge  $e_T^*$ ; the method is discussed in detail on Refs. 12 and 24.

Most of our attempts were restricted to calculations with a cutoff energy of 12 Ry and 3 "special k-points" sampling of the Brillouin zone, and we do not consider them sufficiently converged to provide reliable absolute values of  $e_L^*$  and  $e_T^*$ . Nevertheless, all calculations revealed that the effective charges are weaker and show *the same signs* as in GaAs, i.e.,  $e^*(B) > 0$  and  $e^*(P) < 0$ .

The speculations about the anomalous sign of the effective charges are thus not confirmed. Further calcula-

tionis are required which would also provide the absolute values of the charges and, particularly, their behavior with pressure.

## VI. Conclusions

We have studied the lattice dynamics of BP using the Density Functional Theory, norm-conserving pseudopotentials and plane-wave expansions. This procedure describes correctly the undistorted structure of BP in static equilibrium, and our results for lattice constant and bulk modulus are in good agreement with the available experimental results.

Having a good description of the static equilibrium of BP, we have calculated ab initio its phonon frequencies and eigenvectors at high-symmetry points at the Brillouin zone (BZ). At the  $\Gamma$  point of the BZ, our results agree well with those obtained by Raman scattering<sup>[7]</sup>. At X and L points of the BZ, our calculated data are predictions and are meant to supply the missing experimental information.

Finally, we fitted all the available information by a 10-parameter VOSM and obtained the complete phonon dispersion curves in terms of this interpolation scheme. The calculated elastic constants agree with the experimental ones within  $\approx 4\%$ .

Our attempts at evaluation of the effective charges have shown that the longitudinal effective charges are fairly small, and did not confirm the speculations about the signs: for both  $\epsilon_L^*$  and  $\epsilon_T^*$  we obtained  $\epsilon^*(B) > 0$  and  $\epsilon^*(P) < 0$ .

## References

1. O. R. Golikova, *Pliys. Status Solidi (a)* **51**, 11 (1970).
2. Y. Kumashiro, *J. Mater. Res.* **5**, 2933 (1990).
3. It. M. Wentzcovitch, K. J. Chang and M. L. Cohen, *Phys. Rev.* **B34**, 1071 (1986).
4. R. M. Wentzcovitch, M. L. Cohen and E. K. Lam, *Phys. Rev.* **B36**, 6058 (1987).
5. R. Orlando, R. Dovesi, C. Roetti and V. R. Saunders, *J. Phys.: Condens. Matter* **2**, 7769 (1990).
6. H. W. Leite Alves and K. Kunc, *J. Phys.: Condens. Matter* **4**, 6603 (1992).
7. *Landolt-Bornstein: Numerical Data and Functional Relationship in Science and Technology, New Series*, ed. O. Madelung (Springer-Verlag, Berlin, 1982) Vol. 17a; ed. O. Madelung (Springer-Verlag, Berlin, 1989) Vol. 22a.
8. J. A. Sanjurjo, E. López-Cruz, P. Vogl and M. Cardona, *Phys. Rev.* **B28**, 4579 (1983).
9. I. Hohenberg and W. Kohn, *Phys. Rev.* **136**, B864 (1964); W. Kohn and L. J. Sham, *Phys. Rev.* **140**, A1133 (1965); L. J. Sham and W. Kohn, *Pliys. Rev.* **145**, B561 (1966).
10. G. B. Bachelet, D. R. Hamann and M. Schluter, *Phys. Rev.* **B26**, 2314 (1982).
11. D. M. Ceperley and B. I. Alder, *Phys. Rev. Lett.* **45**, 566 (1980); J. Perdew and A. Zunger, *Phys. Rev.* **B23**, 5048 (1981).
12. See e.g. K. Kunc, *Electronic Structure, Dynamics and Quantum Structural Properties of Condensed Matter*, edited by J. T. Devreese and P. E. van Camp (Plenum Press, New York, 1985) p. 227.
13. K. Kunc and H. Bilz, *Solid State Commun.* **19**, 1027 (1976).
14. T. Suzuki, T. Yagi and S. Akimoto, *J. Appl. Phys.* **54**, 748 (1983).
15. W. Wettleling and J. Windscheif, *Solid State Commun.* **50**, 33 (1984).
16. M. L. Cohen and J. R. Chelikowsky, *Electronic Structure and Optical Properties of Semiconductors*, edited by M. Cardona, P. Fulde, K. von Klitzing and H.-J. Queisser (Springer-Verlag, Berlin, 1988).
17. K. Kunc and R. M. Martin, *Ab-initio Calculation of Phonon Spectra*, edited by J. T. Devreese, V. E. van Doren and P. E. van Camp (Plenum Press, New York, 1983) p. 65.
18. C. O. Rodriguez and K. Kunc, *J. Phys. C: Solid State Phys.* **21**, 5933 (1988).
19. N. Churcher, K. Kunc and V. Heine, *J. Phys. C:*

- Solid State Phys. **19**, 4413 (1986).
20. C. Cheng, K. Kunc and V. Heine, Phys. Rev. **B39**, 5892 (1989).
21. R. G. Dick and A. W. Overhauser, Phys. Rev. **112**, 90 (1958).
22. W. Cochran, *CRC Critical Review in Solid State Sci.* **2**, 1 (1971) and references there in.
23. H. Bilz and W. Kress, *Phonon Dispersion Relations in Insulators*, edited by M. Cardona, P. Fulde and H.-J. Queisser (Springer-Verlag, Berlin, 1979) p. 101.
24. R. M. Martin and K. Kunc, Phys. Rev. **B24**, 2081 (1981).